JOURNAL OF COMPUTATIONAL PHYSICS 116, 160–172 (1995)

Adaptive Approximation of Solutions to Problems with Multiple Layers by Chebyshev Pseudo-Spectral Methods*

ALVIN BAYLISS, ANDREAS CLASS,† AND BERNARD J. MATKOWSKY

Department of Engineering Sciences and Applied Mathematics, Northwestern University, Evanston, Illinois 60208

Received January 18, 1994; revised June 30, 1994

We develop and analyze a family of mappings which enhance the accuracy of Chebyshev pseudo-spectral methods in approximating functions with multiple regions of localized rapid variation (layers). The mapping family depends on $3N - 1$ free parameters, where N is the number of layers. N parameters depend upon the locations of the layers and on the widths of the layers, while the other $N - 1$ parameters depend on the resolution of each layer relative to the first layer. The parameters can be determined adaptively by minimizing a functional which measures the error of the approximation. Techniques to simplify the minimization process are developed. We further demonstrate that the appropriate choice of mappings can lead to a significant reduction in the condition number of matrices associated with Chebyshev pseudo-spectral differentation. We illustrate the effectiveness of the proposed mapping and adaptive procedure by examples in which we approximate (i) given functions exhibiting multiple layers and (ii) the solution of a system of partial differential equations modeling combustion in counterflowing jets so that two distinct flames occur.

1. INTRODUCTION

Chebyshev pseudo-spectral methods have been employed in the solution of partial differential equations occurring in a wide variety of application areas. These methods have been shown to offer significant benefits in accuracy over other methods, such as finite difference methods, when the solution is sufficiently smooth. However, the accuracy of these methods tends to be degraded when approximating solutions which exhibit localized regions of rapid variation (layers). Such problems occur in many areas of application, such as combustion, fluid dynamics, solidification, solid mechanics, and wave propagation, to name but a few. In particular, Chebyshev pseudo-spectral approximations to such functions may exhibit spurious oscillations which can lead to nonlinear instabilities or spurious predictions of solution behavior.

In previous work, it has been shown that the use of appropriately chosen mappings can allow the benefits of Chebyshev pseudo-spectral methods (high accuracy) to be realized for problems in which there is either a single layer or multiple, closely spaced layers, e.g., [3, 7, 15]. The use of such mappings is an essential feature of the adaptive pseudo-spectral method which has been used to compute solutions to a large class of problems in combustion and other areas [1, 3–6, 14, 15]. In this method a prescribed family of mappings, depending on a small number of free parameters, is employed to transform the independent variable or variables of the partial differential equation. As time evolves specific mappings are adaptively chosen from this family by minimizing a functional of the solution which measures the error in the approximation. The effect of each mapping is to represent the solution in a computational coordinate system in which it varies more gradually. Equivalently, the mapping introduces new basis functions that are suitable for the approximation of functions exhibiting layer behavior. The adaptive pseudo-spectral method allows the benefits of pseudo-spectral methods, e.g., high accuracy, to be realized for problems where rapid spatial variations occur.

A crucial element of this method is the choice of the family of mappings employed. The mappings proposed previously have been primarily designed for functions which exhibit either a single layer or several closely spaced layers which are effectively treated as a single layer. In this paper we address the problem of approximating functions exhibiting multiple, widely separated layers.

The accurate resolution of functions exhibiting layer type behavior is particularly important in combustion. Typically, the activation energies of the chemical reactions occurring in combustion are large. As a result the chemical reaction terms are significant only in narrow regions termed reaction zones. In the limit of infinite activation energy, reaction zones shrink to surfaces termed flame fronts, across which certain jump conditions hold. While the flame front model is well suited for mathematical analysis (e.g., [18]), numerical computations are generally conducted for the case of finite (but large) activation energy where the flame occupies a region of non-zero (but small) thickness. In this case the solution is a smooth function, with large gradients across the narrow reaction zone.

In many applications the solution can exhibit multiple layers. In combustion, for example, there can be multiple reaction

* Supported in part by NSF Grants MMS 91-02981 and DMS 93-01635 and DOE Grant DEFG02ER25027.

† Permanent address: IATF, Kernforschungszentrum Karlsruhe GmbH, Karlsruhe, Germany.

0021-9991/95 $6.00

zones associated, e.g., with the production of intermediate species via multiple reaction mechanisms, e.g., [24]. Another example, considered in this paper, is that of flames in counterflowing jets. In this case there are two opposing jets of a premixed combustible mixture resulting in two distinct, although possibly interacting, flames. Such flames have been studied experimentally to reveal the role of flame stretch on flame patterns and dynamics [16]. We note that other physical mechanisms can also lead to multiple layers, for example, in filtration combustion (e.g., [19]).

In order to employ the adaptive pseudo-spectral method for such problems it is necessary to develop methods to resolve functions exhibiting multiple layers, which need not be closely spaced. The primary objective of this paper is to describe an extension of the family of mappings presented in [7] to account for an arbitrary number of layers. Such an extended family involves additional parameters. In fact, if there are N layers, the mapping family we propose has $3N - 1$ free parameters which must be determined. These parameters can be naturally divided into N parameters related to the locations of the layers, N parameters related to the widths of the layers, and $N - 1$ parameters related to the resolution of each layer relative to the first layer. While all of these parameters can in principle be determined by the same minimization problem considered in [3] for the case of a two-parameter mapping, we propose techniques to simplify the minimization problem. In Section 2 we describe the numerical method. In Section 3 we present results, both for the approximation of prescribed functions exhibiting two layers, as well as for the approximation of solutions to a system of partial differential equations modeling combustion in counterflowing jets. We remark that the application of Chebyshev pseudo-spectral methods to problems with two layers, with the ensuing benefit of spectral accuracy, is made feasible due to the proposed family of mappings.

In Section 4 we consider the effect of the mappings on the conditioning of the resulting differentiation matrices. The results demonstrate that for a large range of parameter space the mappings can serve to reduce the condition number of the associated differentiation matrices and thereby the resulting round off error in implementing pseudo-spectral methods. The overall error can be reduced even for functions which do not exhibit layer behavior.

2. NUMERICAL METHOD

We first describe the standard pseudo-spectral method. This description will be brief, since details can be found in [8, 10, 13]. For concreteness we consider a generic one-dimensional evolution equation

$$u_t = u_x + u_{xx} + R(u), \tag{1}$$

where $R(u)$ represents a nonlinear term not involving derivatives. We assume that the problem has been scaled to the interval I, $\{-1 \leq x \leq 1\}$. The solution is approximated by expanding u as a finite sum of Chebyshev polynomials

$$u \simeq u_J \equiv \sum_{j=0}^{J} a_j T_j(x). \tag{2}$$

In the pseudo-spectral method the expansion coefficients a_j are obtained from collocation; that is, the function u_J is forced to solve (1) at a set of $J + 1$ collocation points x_j. The unknowns of the problem are the values u_J at x_j. Pseudo-spectral methods are particularly well suited to nonlinear problems because the nonlinearities are evaluated directly in terms of function values at the collocation points. The expansion (2) is used only for the purposes of computing spatial derivatives. Typically the collocation points are the Gauss–Lobatto points,

$$x_j = \cos(j\pi/J) \quad (j = 0, ..., J).$$

The major advantage of pseudo-spectral methods over finite difference methods is that they can exhibit enhanced accuracy for a fixed number of computational degrees of freedom. In fact, pseudo-spectral methods exhibit infinite order accuracy. That is, the error $e = u - u_J$ satisfies, in an appropriate norm,

$$\|e\| = O(J^{-r}) \tag{3}$$

for all $r \geq 0$ and sufficiently differentiable functions u [10]. The constants involved in the order relation in (3) depend upon the size of the derivatives of u. This is in contrast to finite difference methods where the error is of a fixed order, for example, $O(J^{-2})$ for a second-order method. In practice, spectral methods have been shown to be significantly more accurate than finite difference methods for a variety of problems in areas such as fluid dynamics and meteorology [8, 10, 13].

Pseudo-spectral methods are, however, prone to inaccuracies and oscillations when used to approximate functions which exhibit layers, i.e., localized regions of rapid variation. The approximation of such functions can often be improved by employing mappings. Specifically, assume that a family of mappings,

$$x = q(s, \boldsymbol{\alpha}), \tag{4}$$

is introduced. Here x represents the physical coordinate, $-1 \leq s \leq 1$ is the transformed (computational) coordinate, and $\boldsymbol{\alpha}$ denotes parameters to be determined in the course of the computation. The pseudo-spectral method can then be applied to the transformed equation to approximate the transformed function $u(q(s, \boldsymbol{\alpha}), t)$. We note that the effect of the mapping can be regarded as transforming the function to be approximated by the expansion (2) from $u(x)$ to the (hopefully) more gradually varying $u(q(s, \boldsymbol{\alpha}))$. An alternative interpretation is to transform

the basis functions from $T_n(s)$ to the (hopefully more suitable) $T_n(q^{-1}(x, \boldsymbol{\alpha}))$.

In [7] a family of mappings was presented which was shown to be very effective in approximating functions exhibiting a single layer or multiple closely spaced layers. It is instructive to describe the inverse mapping

$$s = q^{-1}(x, \boldsymbol{\alpha}) = s_0 + \tan^{-1}(\alpha_{11}(x - \alpha_{12}))/\lambda, \tag{5}$$

where α_{11} and α_{12} are parameters determining individual members of the mapping family, while s_0 and λ are determined so that (5) maps the interval I univalently onto itself. In order for our notation to be readily extendable to the case of multiple layers, we employ a double index notation for $\boldsymbol{\alpha}$, where the first index refers to the layer and the second index refers to parameters associated with the layer.

In order to see that the inverse function $s = q^{-1}(x, \boldsymbol{\alpha})$ is a suitable mapping to transform functions exhibiting layer behavior to more gradually varying functions, we note that (5) itself exhibits layer behavior and the composite function $q^{-1}(q(s, \boldsymbol{\alpha}), \boldsymbol{\alpha}) = s$ is gradually varying. This suggests that for a function exhibiting layer behavior the composite function will be gradually varying, provided $\boldsymbol{\alpha}$ is properly chosen. As a mapping the effect of (5) is to expand a region around the point $x = \alpha_{12}$ of width approximately α_{11}^{-1} and compress the remainder of I. Thus in terms of approximating a given function the parameters α_{11} and α_{12} can be interpreted as the inverse width and the location of the layer, respectively.

In the solution of partial differential equations, these properties of the solution are generally not known in advance and may change during the course of the computation. A procedure to determine $\boldsymbol{\alpha}$ adaptively was presented in [3, 5]. In this adaptive procedure $\boldsymbol{\alpha}$ is determined so as to minimize a functional of the solution which measures the error in the approximation of the solution by its Chebyshev expansion. The functional,

$$I_2(g) = \left(\int_{-1}^{1} (\mathcal{L}^2 g)^2 / w(s)\, ds \right)^{1/2}, \tag{6}$$

where

$$w(s) = \sqrt{1 - s^2}, \quad \mathcal{L} = w(s)\, d/ds,$$

derived in [3] has been shown to be an effective measure of this approximation error. In the adaptive pseudo-spectral method (6) is evaluated for different values of $\boldsymbol{\alpha}$ until a minimum is found. The integral in (6) is evaluated in the physical coordinate x by an explicit change of variable, making use of the fact that the derivative of the mapping can be computed explicitly. It has been shown in [14] that (6) is equivalent to the functional $\pi/2 \sum_{j=0}^{\infty} c_j (j a_j)^2$, where a_j is the coefficient of T_j in the Chebyshev expansion of g and $c_0 = 2$, $c_j = 1$, $j > 0$. In addition to the family of mappings there are other important aspects of the adaptive procedure such as the mechanism by which a search for a new coordinate system is triggered and the relationship between the timestep and the mapping is chosen. These aspects have been described in detail in [3, 5] and as the major focus of this paper is the family of mappings, they are omitted here for brevity.

Only a single layer can be expanded by the use of (5), although the results in [7] demonstrate that accurate approximations can be obtained for functions with multiple layers that are closely spaced. In order to deal with multiple layers that are widely separated it is necessary to extend the mapping family (5). For simplicity we first consider the case of two layers. In this case the extended family of mappings is

$$\begin{aligned} s = q^{-1}(x, \boldsymbol{\alpha}) = s_0 + (&\tan^{-1}(\alpha_{11}(x - \alpha_{12})) \\ &+ \tan^{-1}(\alpha_{21}(x - \alpha_{22})))/\lambda, \end{aligned} \tag{7}$$

where for the ith layer α_{i1} and α_{i2} are parameters to be determined and s_0 and λ are determined so that (7) maps the interval I univalently onto itself,

$$s_0 = \frac{\kappa_1 - \kappa_2}{\kappa_1 + \kappa_2}, \quad \lambda = (\kappa_1 + \kappa_2)/2,$$

where

$$\begin{aligned} \kappa_1 &= \tan^{-1}(\alpha_{11}(1 + \alpha_{12})) + \tan^{-1}(\alpha_{21}(1 + \alpha_{22})), \\ \kappa_2 &= \tan^{-1}(\alpha_{11}(1 - \alpha_{12})) + \tan^{-1}(\alpha_{21}(1 - \alpha_{22})). \end{aligned}$$

It is clear from (7) that α_{i2}, $i = 1, 2$, specify the locations of the layers, while α_{i1}, $i = 1, 2$, specify the inverse widths of the layers. We note that (7) reduces to (5) when $\alpha_{21} = \alpha_{11}$ and $\alpha_{22} = \alpha_{12}$. The construction of (7) is motivated by the notion of adding two layers, a technique commonly employed in the mathematical analysis of problems exhibiting layer behavior.

We note that (7) affords the same overall resolution to both layers. It is possible to extend the mapping family to allow for differing resolution of each layer. This can be done by the mapping family

$$\begin{aligned} s = q^{-1}(x, \boldsymbol{\alpha}) = s_0 + (&\alpha_{13} \tan^{-1}(\alpha_{11}(x - \alpha_{12})) \\ &+ \alpha_{23} \tan^{-1}(\alpha_{21}(x - \alpha_{22})))/\lambda, \end{aligned} \tag{8}$$

where without loss of generality we can take $\alpha_{13} = 1$ so that α_{23} is a measure of the resolution for the second layer relative to the first layer. In the numerical computations presented here we consider only the case of (7), i.e., $\alpha_{23} = 1$.

In applications it is necessary to evaluate the mapping rather than the inverse mapping, i.e., to solve for x given s, where s is typically one of the Gauss–Lobatto points. While this can always be done numerically, for the special case of (7) (i.e., for two layers with $\alpha_{23} = 1$) it is possible to evaluate the

mapping explicitly by employing trigonometric identities. Specifically, we have

$$x = b \pm \sqrt{z_1 + z_2}, \tag{9}$$

where

$$b = (\alpha_{12} + \alpha_{22}) - \tau(1/\alpha_{21} + 1/\alpha_{11}),$$

$$\tau = \cot(\lambda(s - s_0)),$$

$$z_1 = ((\alpha_{12} - \alpha_{22}) + \tau(1/\alpha_{21} - 1/\alpha_{11}))^2,$$

$$z_2 = 4(1 + \tau^2)/(\alpha_{11}\alpha_{21}).$$

The choice of sign in (9) depends on the sign of τ. In addition, an expansion can be derived for $\lambda(s - s_0)$ near 0, where $\tau \to \pm\infty$, depending on the sign of $s - s_0$. If $w = \lambda(s - s_0)$ then for $|w|$ sufficiently small we have

$$x = \tilde{x}_0 + \tilde{x}_1 w + \tilde{x}_2 w^2,$$

where

$$\tilde{x}_0 = (\alpha_{11}\alpha_{12} + \alpha_{21}\alpha_{22})/(\alpha_{11} + \alpha_{21}),$$

$$\tilde{x}_1 = 1/(\alpha_{11} + \alpha_{21}) + (\alpha_{11}\alpha_{21}(\alpha_{12} - \alpha_{22}))^2/(\alpha_{11} + \alpha_{21})^3$$

and

$$\tilde{x}_2 = \tilde{x}_1\alpha_{11}\alpha_{21}(\alpha_{11} - \alpha_{21})(\alpha_{12} - \alpha_{22})/(\alpha_{11} + \alpha_{21})^2.$$

The implementation of (7) within the adaptive pseudo-spectral method requires the adaptive determination of four parameters (α_{ij}, $i, j = 1, 2$). In principle this can be done by varying these parameters and minimizing (6) for either one of the unknowns or for a combination of the unknowns of the problem. In many instances approximate techniques can be employed to reduce the order of this minimization problem. For example, it is often the case that the locations of the layers can be determined from functionals of the solution, without recourse to a minimization procedure. This can be done, for example, by locating extrema of the second derivatives of the dependent variables. In many combustion problems it is possible to determine the locations of the reaction zones by determining maxima of the reaction term, as this characterizes the flame. We have incorporated such techniques into our combustion computations and do not include α_{12} and α_{22} in the minimization. In addition, it is often possible to decouple the minimization problem for α_{11} and α_{21} into two minimization problems for α_{11} and α_{21} separately. We note that α_{11} and α_{21} represent the widths of two layers, and if the layers are sufficiently separated, these parameters are not strongly coupled. We first keep α_{21} fixed at its old value and minimize (6), varying only α_{11}. We then keep α_{11} fixed and minimize, varying only α_{21}. This process is then iterated until convergence is attained. In all computations that we have performed at most five iterations have been required.

In two-dimensional calculations $\boldsymbol{\alpha}$ can be chosen to be a function of a transverse coordinate, leading to a fully two-dimensional mapping. An alternative is to choose $\boldsymbol{\alpha}$ independent of the transverse coordinate by averaging over all the transverse directions. The first approach is described in detail in [4]. This method requires the evaluation of additional terms in the equation and is more costly for each timestep. In the two-dimensional computations presented here the use of average values of $\boldsymbol{\alpha}$ is sufficient to illustrate the nonplanar structure of the flame and the effectiveness of the proposed mapping family.

The family (8) can be readily extended to account for more than two layers. If N layers are to be accounted for we have

$$s = q^{-1}(x, \boldsymbol{\alpha}) = s_0 + \left(\sum_{i=1}^{n} \alpha_{i3}\tan^{-1}(\alpha_{i1}(x - \alpha_{i2}))\right)/\lambda, \tag{10}$$

where s_0 and λ are suitably determined so that the resulting mapping maps I univalently onto itself and α_{i3} is a measure of the resolution for the ith layer relative to the first layer ($\alpha_{13} = 1$). For completeness we give expressions for s_0 and λ for (10),

$$s_0 = (S_- - S_+)/(S_- + S_+), \quad \lambda = (S_- + S_+)/2,$$

where

$$S_\pm = \left(\sum_{i=1}^{n} \alpha_{i3}\tan^{-1}(\alpha_{i1}(1 \pm \alpha_{i2}))\right).$$

Finally we note that other functions exhibiting similar behavior, for example tanh, can be incorporated within the methodology described above to created other families of mappings suitable for multiple layers.

3. ACCURACY

We first consider the effectiveness of the mapping family (7) in approximating given functions exhibiting two separated layers. We consider maximum norms for the errors in approximating the function u and itrs first two derivatives by a Chebyshev expansion in the transformed coordinate, i.e., $u \simeq u_J(s)$. Thus in the physical coordinate x the approximation is $u_J(q^{-1}(x, \boldsymbol{\alpha}))$. The Chebyshev polynomial approximation $u_J(s)$ is obtained from collocation at the points

$$s_j = \cos(\pi j/J'), \quad j = 0, ..., J'. \tag{11}$$

The errors are defined as

$$E_0 = \max_{0\le j\le J'} (|u(x_j) - u_J(q^{-1}(x_j, \boldsymbol{\alpha}))|),$$

$$E_1 = \max_{0\le j\le J} (|u'(x_j) - u_J'(q^{-1}(x_j, \boldsymbol{\alpha}))|),$$

$$E_2 = \max_{0\le j\le J} (|u''(x_j) - u_J''(q^{-1}(x_j, \boldsymbol{\alpha}))|),$$

where for E_1 and E_2 the maximum is taken over the points

$$x_j = q(s_j, \boldsymbol{\alpha}), \quad s_j = \cos(\pi j/J), \quad j = 0, ..., J, \tag{12}$$

(i.e., the image of the points (11) under the mapping), while for E_0 the maximum is taken over the points

$$x_j = q(s_j, \boldsymbol{\alpha}), \quad s_j = \cos(\pi j/J'), \quad j = 0, ..., J',$$

where $J' \gg J$ (we note that by construction $u(x) - u_J(q^{-1}(x_j, \boldsymbol{\alpha})) = 0$ at the points (12)).

In order to assess the effectiveness of the proposed mappings it is important to demonstrate both the ability of the mappings to yield accurate approximations to functions exhibiting multiple layers and the ability of the adaptive procedure to determine appropriate parameters of the mappings for problems with multiple layers. We have therefore designed our numerical experiments to simulate the adaptive procedure as we have implemented it for combustion problems. Specifically, since the locations of the reaction zones can be estimated from maxima of the reaction rate terms, α_{12} and α_{22} can be estimated without resorting to a minimization procedure. In our approximation results we specify these parameters beforehand. The parameters α_{11} and α_{21} are obtained by successive minimizations, so that we first minimize (6) with respect to α_{11}, then with respect to α_{21}, and iterate until the results of the minimization do not change. In practice at most five iterations are required for all of the cases considered here.

We have found that (6) tends to somewhat overestimate the parameters α_{11} and α_{21} (a somewhat similar, but less pronounced, tendency was observed in [7] for the case of a single layer). We believe that one reason for this in the two-layer case is that in the minimization the layers compete for more resolution; i.e., there is a tendency for each layer to try to increase its resolution at the expense of the other layer, thereby leading to overpredictions of the inverse width parameters. In order to compensate for this we modify (6) by adding a penalty term which increases with α_{11} and α_{21}, specifically the term $\gamma(\alpha_{11} + \alpha_{21})$, to (6). All results presented below were obtained with $\gamma = 1$. This does not always give the most accurate approximation; in general, smaller errors can be obtained by scanning the accuracy of the approximation as α_{11} and α_{21} are varied. However, since the exact solution is not known in partial differential equation applications, we illustrate the accuracy that can be expected from a fixed adaptive procedure, as would be employed in the solution of partial differential equations. We note that it is also possible to split the domain into two subdomains, each encompassing one layer, and minimize (6) separately for each subdomain.

We consider the approximation of functions exhibiting multiple layers, specifically,

$$u(x) = \tanh(\sigma_1(x - x_1)) + \delta\tanh(\sigma_2(x - x_2)) \tag{13}$$

and

$$u(x) = \exp(-(\sigma_1(x - x_1))^2/2) + \delta\exp(-(\sigma_2(x - x_2))^2/2). \tag{14}$$

Results for illustrative values of δ, σ_1, σ_2, x_1, and x_2 are presented in Table I for (13) and in Table II for (14). In the approximations we use $J' = 350$ and $J = 120$, except where noted. We specify beforehand that $\alpha_{12} = x_1$ and $\alpha_{22} = x_2$. The parameters α_{11} and α_{21} are obtained by minimization of (6) with the added penalty term $\gamma(\alpha_{11} + \alpha_{21})$ over a grid with spacing $\Delta\alpha_{11} = \Delta\alpha_{21} = 1$. A more accurate minimization is not needed in practice. Entries with "U" in the columns corresponding to mapping parameters, indicate that no mapping was employed. The different cases illustrated in the tables are distinguished by a case identifier (ID).

The parameters are chosen so that the layer regions for (14) are generally narrower than for (13), and consequently the approximation for (14) is more sensitive to values of α_{11} and α_{21} than for (13). In all computations the penalty term coefficient $\gamma = 1$. We point out that all errors can be reduced by tuning γ; i.e., the limiting factor on accuracy is not the resolving power of the family of mappings (7) but rather the ability of (6) with the penalty term to select truly optimal mapping parameters for cases with multiple layers. In using this method to solve systems of partial differential equations, this parameter can be chosen by experiment for the particular problem under consideration; however, in both the approximation and combustion cases presented here we have chosen to present the results with the fixed value of $\gamma = 1$.

The results in Tables I and II demonstrate that the mappings (7) allow dramatic improvements in the approximation by Chebyshev pseudo-spectral expansions of functions with multiple layers. Indeed, the mappings make the use of Chebyshev pseudo-spectral methods for such functions feasible. We can also infer from these results the properties of, and the problems associated with, the adaptive Chebyshev pseudo-spectral approximation of functions with multiple layers. The first case in each table, cases C11 and C21, respectively, is an example where the layers are of equal size and thickness. In this case the adaptive procedure selects $\alpha_{11} = \alpha_{21}$ as would be expected to resolve two identical layers. In order to demonstrate the number of points required for comparable accuracy without mappings, errors for the unmapped case with $J = 480$ are given (cases C12 and C22, respectively).

TABLE I

Results for Approximating $u(x) = \tanh(\sigma_1(x - x_1)) + \delta \tanh(\sigma_2(x - x_2))$

δ	x_1	x_2	σ_1	σ_2	α_{11}	α_{21}	E_0	E_1	E_2	ID
1.0	−0.5	0.5	50.	50.	U	U	2.75×10^{-2}	4.55×10^{0}	2.91×10^{2}	C11
1.0	−0.5	0.5	50.	50.	19.	19.	1.83×10^{-9}	1.05×10^{-7}	2.76×10^{-5}	C11
1.0	−0.5	0.5	50.	50.	U	U	6.29×10^{-8}	3.87×10^{-5}	2.85×10^{-2}	C12
0.5	−0.5	0.5	50.	50.	19.	13.	1.17×10^{-9}	7.18×10^{-7}	4.14×10^{-4}	C13
0.1	−0.5	0.5	50.	50.	20.	6.	7.68×10^{-6}	2.45×10^{-3}	5.25×10^{-1}	C14
1.0	−0.5	0.5	50.	25.	19.	11.	1.23×10^{-9}	3.03×10^{-7}	1.31×10^{-4}	C15
0.1	−0.5	0.5	50.	25.	20.	3.	3.20×10^{-6}	5.49×10^{-4}	1.70×10^{-1}	C16
10.0	−0.5	0.5	50.	25.	14.	16.	2.60×10^{-6}	3.89×10^{-4}	1.66×10^{-1}	C17
1.0	−0.9	0.0	50.	50.	15.	18.	1.84×10^{-10}	2.32×10^{-8}	9.79×10^{-6}	C18

The major problem revealed is that of a degradation in accuracy when the amplitudes of the two layers differ significantly. For the examples considered here, this degradation does not become apparent until the amplitudes of the layers differ by an order of magnitude. This can be seen by comparing case C13 (C23), where $\delta = 0.5$, with case C14 (C24), where $\delta = 0.1$. We have determined that this is more of a deficiency of the adaptive choice of parameters rather than of the mapping itself. For these cases each layer has the same thickness (determined by σ_1 and σ_2) and the most accurate approximations would occur for $\alpha_{11} = \alpha_{21}$. For example, for (13) specifying $\alpha_{11} = \alpha_{21} = 19$ with $\delta = 0.1$ leads to accuracy comparable to that obtained when $\delta = 1.0$ and similarly for (14). Since the functional (6) is a global functional, the effect of the minimization is to force a reduction of the resolution of the smaller amplitude layer with a corresponding increase in the resolution of the larger amplitude layer. We note that in many instances it is possible to know beforehand that the amplitudes of the layers differ significantly, and thus compensate by either modifying the penalty term or possibly splitting the domain into two subdomains and minimizing over each subdomain. We do not do this here, as we focus on the properties of the mapping family with a fixed adaptive procedure to determine the parameters.

In cases C15, C16, C17 (C25, C26, C27) we consider the approximation of two layers of differing thickness ($\sigma_2/\sigma_1 = 0.5$). The data indicates both that the mapping can resolve layers of differing thicknesses and that the adaptive procedure can distinguish the differing thicknesses as long as the broad layer does not have a significantly greater amplitude than the narrower layer. When $\delta = 10$, the adaptive procedure forces excessive resolution of the broader layer, thus degrading the overall accuracy. This is again due to the global nature of the functional (6) and can also be accounted for by modifying the penalty term or by splitting the domain for the evaluation of (6), should it be known in advance that the amplitudes of the layers are sufficiently out of scale.

It has been shown previously that Chebyshev approximations are more accurate for boundary layers than for interior layers [7, 21]. Consequently smaller values of α_{11} or α_{21} should be required when the corresponding layers are close to the boundaries. The results with one of the layers close to the boundary point $x = -1$ (cases C18 and C28, respectively) demonstrate that minimization of the functional (6) does indeed detect differing resolution requirements depending on the location of the layer, producing a larger value for α_{21} for the layer located at $x = 0$.

Finally, we point out that we have examined the case of a single layer ($\delta = 0$), employing the mapping (5), designed

TABLE II

Results for Approximating $u(x) = \exp(-(\sigma_1(x - x_1))^2/2) + \delta \exp(-(\sigma_2(x - x_2))^2/2)$

δ	x_1	x_2	σ_1	σ_2	α_{11}	α_{21}	E_0	E_1	E_2	ID
1.0	−0.5	0.5	100.	100.	U	U	1.53×10^{-1}	2.57×10^{1}	4.33×10^{4}	C21
1.0	−0.5	0.5	100.	100.	30.	30.	3.43×10^{-8}	1.69×10^{-5}	5.34×10^{-3}	C21
1.0	−0.5	0.5	100.	100.	U	U	4.88×10^{-8}	2.78×10^{-5}	1.47×10^{0}	C22
0.5	−0.5	0.5	100.	100.	30.	21.	3.26×10^{-8}	9.48×10^{-6}	4.79×10^{-3}	C23
0.1	−0.5	0.5	100.	100.	32.	9.	1.29×10^{-6}	5.46×10^{-4}	1.48×10^{-2}	C24
1.0	−0.5	0.5	100.	50.	30.	18.	1.20×10^{-7}	2.97×10^{-5}	6.60×10^{-3}	C25
0.1	−0.5	0.5	100.	50.	32.	5.	2.26×10^{-8}	9.72×10^{-6}	8.35×10^{-3}	C26
10.0	−0.5	0.5	100.	50.	20.	32.	3.40×10^{-5}	1.88×10^{-2}	1.07×10^{1}	C27
1.0	−0.9	0.0	100.	100.	26.	29.	1.49×10^{-8}	8.86×10^{-6}	5.28×10^{-3}	C28

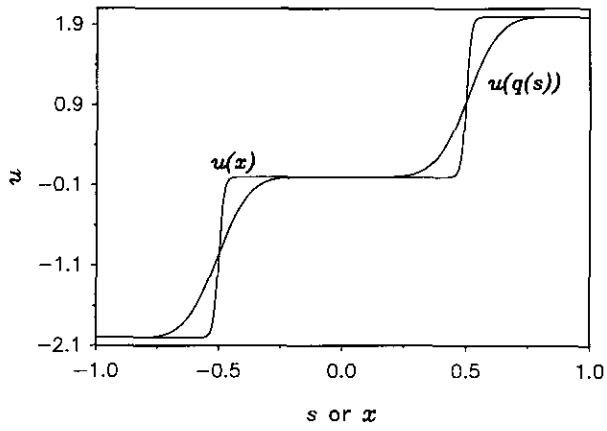

FIG. 1. Equation (13) plotted as a function of both s and x. Parameters are as in the second entry in Table I.

for functions exhibiting single layer behavior. Employing 61 collocation points we find results very similar to those obtained in Tables I and II for the two layer case with $\delta = 1$ and with 121 collocation points. These results indicate that with the appropriate choice of mappings the accuracy of the approximation of similar layers roughly scales with the number of collocation points per layer. In Figs. 1 and 2 we plot (13) and (14) respectively as both functions of x and s. In each case the function and the mapping are those associated with the second row in Tables I and II, respectively.

The penalty term $\gamma(\alpha_{11} + \alpha_{21})$ is important in preventing excessive resolution of each layer. The choice $\gamma = 1$ employed for all calculations presented here appears reasonably effective in controlling this phenomenon in the determination of mapping parameters. No attempt has been made to tune γ for each case. The accuracy of the approximation is robust to changes in γ. In order to illustrate this we consider the approximation for the case C16, where both the amplitudes and thicknesses of the

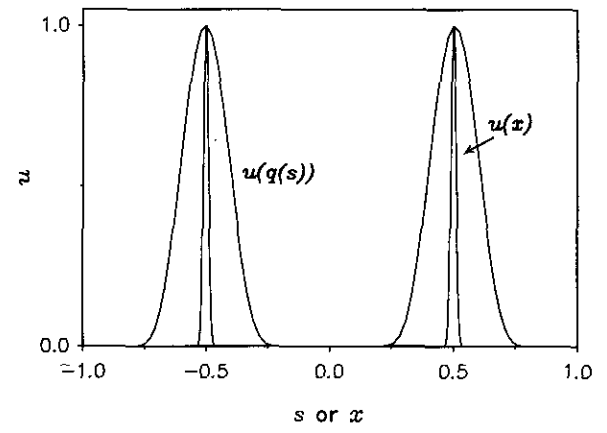

FIG. 2. Equation (14) plotted as a function of both s and x. Parameters are as in the second entry in Table II.

TABLE III

Effect of γ on the Approximation of Case C16

γ	α_{11}	α_{21}	E_0	E_1	E_2
1.0	20.	3.	3.20×10^{-6}	5.49×10^{-4}	1.70×10^{-1}
0.5	26.	4.	1.98×10^{-7}	4.45×10^{-5}	1.21×10^{-2}
1.5	16.	2.	3.15×10^{-5}	4.54×10^{-3}	4.53×10^{0}

two layers are highly disparate and the errors listed in Table I are relatively large compared to most of the other cases. In Table III we illustrate the errors for three different values of γ. For this case increased accuracy is obtained for values of $\gamma < 1$. Increasing γ leads to a reduction in α_{11} and α_{21}, in particular leading to significantly reduced resolution of the thicker layer. All of these results are orders of magnitude smaller than for the unmapped case. In solving partial differential equations it is often possible to identify poor choices of parameters, for example by oscillations in the solution, and to improve the computation by adjusting the calculation of the mapping parameters.

We next illustrate the effect of inaccurate specification of the location parameters α_{12} and α_{22}. In practice the locations of the layers will not be known exactly. For example, the algorithm employed to specify the locations of the interfaces, e.g., in combustion the maxima of the reaction rate terms, might be imprecise. In many cases there may be variations in the flame location with respect to a transverse coordinate or coordinates, e.g., a cellular pattern along the flame front. A general two-dimensional adaptive procedure, in which the parameters are taken as functions of a transverse coordinate is described in [4] and is applicable to the mapping family (7). In many instances, however, the mapped Chebyshev pseudo-spectral is sufficiently accurate that mappings with a single location parameter, taken as the average across the reaction zone, can resolve the nonplanar state.

In order to deal with such problems it is important to understand the robustness of the mapping family (7) with respect to the location parameters α_{12} and α_{22}. We demonstrate the effect of inaccurate specification of these parameters in Table IV. In constructing this table we have fixed $\alpha_{12} = -\alpha_{22} = -0.5$ and have varied the centers of the layers x_1 and x_2. Results are presented for (13) (with $\sigma_1 = \sigma_2 = 50.$) and (14) $\sigma_1 = \sigma_2 = 100.$) with $\delta = 1$.

For these parameters the thickness of each layer is approximately 0.2 for (13) and 0.1 for (14). When 121 collocation points are employed deviations between the layer location and the location parameter of approximately 10% of the layer width can be accomodated before relatively large errors appear in the second derivative. Since for fixed mapping parameters the rapid convergence of spectral methods still occurs [10] a relatively small increase in J can significantly reduce the error, even for the second derivative.

TABLE IV

Results for Imperfectly Approximating Layer Locations

$u(x)$	J	x_1	x_2	α_{11}	α_{21}	E_0	E_1	E_2
(13)	120	−0.525	0.525	17.	17.	5.58×10^{-11}	3.34×10^{-8}	1.36×10^{-5}
(13)	120	−0.475	0.475	17.	17.	6.61×10^{-9}	4.24×10^{-6}	7.28×10^{-4}
(13)	120	−0.45	0.45	13.	13.	6.90×10^{-6}	3.34×10^{-3}	1.02×10^{0}
(13)	160	−0.45	0.45	13.	13.	1.88×10^{-7}	1.11×10^{-4}	1.83×10^{-2}
(14)	120	−0.5125	0.5125	28.	28.	7.90×10^{-11}	5.46×10^{-8}	7.71×10^{-5}
(14)	120	−0.4875	0.4875	27.	27.	1.07×10^{-6}	8.94×10^{-4}	3.39×10^{-1}
(14)	120	−0.475	0.475	23.	23.	2.09×10^{-5}	1.30×10^{-2}	3.98×10^{0}
(14)	160	−0.475	0.475	23.	23.	4.32×10^{-7}	2.32×10^{-4}	1.32×10^{-1}

The first and fifth rows of Table IV are slightly more accurate than the corresponding calculations with $x_2 = -x_1 = 0.5$ (i.e., cases C11 and C21 in Tables I and II, respectively). We believe that this is primarily due to the values of α_{11} and α_{21} chosen by the adaptive procedure. For (13) similar results occur for $x_2 = -x_1 = 0.535$. As the locations of the layers move further from ± 0.5 the errors increase, as would be expected. Although we have not extensively studied the error as a function of x_1 and x_2, the computed errors are orders of magnitude below the unmapped case for $x_2 = -x_1 = 0.555$. Similar results (not shown here) have been obtained for $x_2 \neq -x_1$. We note that the errors are smaller when the actual layer locations (x_1 and x_2) satisfy $x_1 < \alpha_{12}$ and $x_2 > \alpha_{22}$, and that it may be advantageous to ensure this in computations. We believe that this is due to insufficient resolution in the mapping (7) in the region between the two layers (i.e., for $\alpha_{12} \leq x \leq \alpha_{22}$) in (7). It is possible that replacement of $\tan^{-1}$ by a different, although similar, function might ameliorate this.

This last point is further emphasized in Table V, where we consider two layers modulated by an oscillatory function; specifically we consider the function

$$u(x) = (1 + \varepsilon \cos(\omega x))(\tanh(\sigma_1(x - x_1)) + \delta \tanh(\sigma_2(x - x_2))). \tag{15}$$

Functions of the form (15) describe two layers modulated by a small scale, global oscillation. We consider the case $\varepsilon = 0.1$, $\sigma_1 = \sigma_2 = 50$, $x_2 = -x_1 = 0.5$, and the approximation is constructed using $J = 120$. In Table V two cases are considered; $\delta = 1.0$ and $\delta = 0.9$ which we denote by the identifiers C51 and C52, respectively.

These cases are chosen to illustrate the behavior of the mapping in approximating layers with a superimposed fine scale structure. We note that (15) is a more severe test than would likely hold in many applications because the modulation is global rather than localized around the layers. For both cases the structure of the modulation is similar for $|x| > 0.5$, i.e., in the region between the layers and the boundaries. However, for $|x| < 0.5$, i.e., in the region between the layers, the resulting function is 0 for $\delta = 1.0$ while it consists of a nonzero modulation for $\delta \neq 1.0$. In both cases the location parameters are specified at the center of the layers, $\alpha_{12} = x_1$, $\alpha_{22} = x_2$, while the parameters α_{11} and α_{21} are chosen as described above.

The functional (6) is sufficiently sensitive to detect the modulation by reducing the resolution of the layers (i.e., α_{11} and α_{21} are reduced from the values that they would have if there were no modulation). Furthermore, the reduction in resolution increases as ω increases as would be expected since the wavelength of the modulation decreases. The errors are considerably larger for case C52. This indicates that the modulation between

TABLE V

Results for Approximating $u(x) = (1 + \varepsilon\cos(\omega x))\ \tanh(\sigma_1 x - x_1)) + \delta\tanh(\sigma_2(x - x_2)$

δ	ω	α_{11}	α_{21}	E_0	E_1	E_2	ID
1.0	10.	17.	17.	2.50×10^{-10}	3.57×10^{-8}	1.78×10^{-5}	C51
1.0	20.	12.	12.	1.23×10^{-8}	7.67×10^{-6}	1.49×10^{-3}	C51
1.0	30.	9.	9.	7.35×10^{-7}	3.43×10^{-4}	1.10×10^{-1}	C51
1.0	40.	8.	8.	4.10×10^{-6}	1.47×10^{-3}	4.52×10^{-1}	C51
1.0	10.	18.	16.	4.62×10^{-4}	3.36×10^{-2}	9.33×10^{0}	C52
1.0	20.	11.	13.	1.42×10^{-3}	3.96×10^{-2}	6.80×10^{0}	C52
1.0	30.	9.	8.	1.39×10^{-3}	5.42×10^{-2}	4.87×10^{0}	C52
1.0	40.	8.	9.	8.39×10^{-3}	3.19×10^{-1}	1.08×10^{1}	C52

the layers and the boundaries is well resolved by the mapping. When there is sufficiently rapid oscillation in the region between the two layers, accuracy is degraded due to the behavior of the mapping family (7) in underresolving this region, an effect which could likely be ameliorated by choice of a different but similar function.

We next illustrate the behavior of the mapping family (7) in the solution of partial differential equations. We consider the problem of combustion in counterflowing jets [16]. In this problem, there are two jets of a premixed combustible mixture emanating from oppositely placed locations. Associated with each jet a flame will form at a certain distance from the jet. Thus two distinct flames will exist. The distance between the flames will depend on the velocity of the jet as well as on parameters of the mixture. Due to the spreading of the jets each flame will be stretched.

We neglect bouyancy effects and consider the diffusional thermal model in which the thermal expansion of the gas is assumed to be weak [18]. In this model the flow field is assumed to be unaffected by the chemical reactions. The transport of heat and species can be computed from a system of advection diffusion equations with the prescribed flow field as a coefficient. We further assume that the reaction is limited by a single deficient component and is governed by one-step, irreversible Arrhenius kinetics.

If dimensional quantities are denoted by $\tilde{}$ the unknowns are the temperature $\tilde{T}$ and the concentration $\tilde{C}$ of the deficient component. $\tilde{T}_u$ and $\tilde{T}_b$ are the temperatures of the unburned and burned gas, respectively. The unburned value of $\tilde{C}$ at one of the jets is $\tilde{C}_u$. The concentration of the deficient component may differ at the opposing jet. Other dimensional quantities are the coefficient of thermal conductivity $\tilde{\lambda}$, the activation energy $\tilde{E}$, and the gas constant $\tilde{R}$. We introduce the nondimensional reduced temperature and nondimensional concentration by

$$\Theta = (\tilde{T} - \tilde{T}_u)/(\tilde{T}_b - \tilde{T}_u), \quad C = \tilde{C}/\tilde{C}_u.$$

The spatial and temporal variables are nondimensionalized by

$$t = \frac{\tilde{t}\tilde{U}^2}{\tilde{\lambda}}, \quad x_i = \frac{\tilde{x}_i\tilde{U}}{\tilde{\lambda}},$$

where $\tilde{U}$ is the planar adiabatic flame speed for the case of infinite activation energy in which the reaction term is replaced by a surface delta function. We employ Cartesian coordinates (x, y) and assume that the opposing jets are both of nondimensional strength K and are located at $x \to \pm\infty$. The nondimensionalized flow velocity is

$$\mathbf{V} = (Kx, -Ky),$$

so that there is stretching of planar flames in the y direction. We note that as K increases combustion occurs closer to the stagnation line $x = 0$. Thus as K increases the two flames will move closer together, resulting in a greater interaction between them.

The equations of the model are

$$\begin{aligned} \Theta_t &= \Delta\Theta - \mathbf{V}\cdot\nabla\Theta + C\Lambda \exp\left(\frac{N(1-\Sigma)(\Theta-1)}{\Sigma + (1-\Sigma)\Theta}\right), \\ C_t &= \frac{\Delta C}{\mathrm{Le}} - \mathbf{V}\cdot\nabla C - C\Lambda \exp\left(\frac{N(1-\Sigma)(\Theta-1)}{\Sigma + (1-\Sigma)\Theta}\right). \end{aligned} \tag{16}$$

Here Δ is the Laplacian, $\Sigma = \tilde{T}_u/\tilde{T}_b$, $N = \tilde{E}/(\tilde{R}\tilde{T}_b)$, Le is the Lewis number, the ratio of thermal to mass diffusivity, and $\Lambda = Z^2/2\mathrm{Le})$, where $Z = N(1-\Sigma)$ is the Zeldovich number. We note that Λ, which is referred to as the flame speed eigenvalue, depends on the nondimensionalization. The value employed above arises from the use of the planar, adiabatic flame velocity in the infinite activation energy limit. A different nondimensionalization would change the spatial and temporal scales but would not alter the basic patterns exhibited by the solution.

The boundary conditions are

$$\begin{aligned} C(\Theta) \to 1\ (0), \quad \text{as } x \to -\infty, \\ C(\Theta) \to \phi\ (0), \quad \text{as } x \to \infty, \end{aligned} \tag{17}$$

so that the concentration of the deficient component at the jet located at $+\infty$ is $\phi\tilde{C}_u$. When $\phi = 1$ there is symmetry across the stagnation line. As ϕ deviates from 1 the degree of asymmetry between the two flames increases. In our computations these boundary conditions are imposed at points $x_{-\infty}$ and x_∞, far from the reaction zone where combustion occurs. The computed results were found to be insensitive to $x_{-\infty}$ and x_∞, provided they were taken sufficiently far from the reaction zone. In the two-dimensional solutions a Fourier method was used on the domain $-y_\infty \le y \le y_\infty$ with symmetry about $y = 0$ imposed. The nonplanar states computed were localized around $y = 0$ and y_∞ was taken sufficiently large so that there was no significant influence of the boundary conditions on the transverse structure of the flame front. The computations were performed at the NCSA and NERSC.

We illustrate the adaptive procedure by both one-dimensional solutions (i.e., solutions independent of y) and solutions exhibiting localized nonplanar states, similar to those found in [11] for the Kuramoto–Sivashinsky equation. In all computations the following parameters were held fixed, $N = 20$, $\Sigma = 0.5$ and $\mathrm{Le} = 0.5$. All solutions reported here are stationary solutions, obtained by solving the time dependent system of partial differential equations until steady state is achieved. The temporal integration is performed using the backward Euler scheme with operator splitting. The reaction term is treated explicitly while all other terms are treated implicitly. The temporal integration method is described in detail in [6]. We employed 141 points

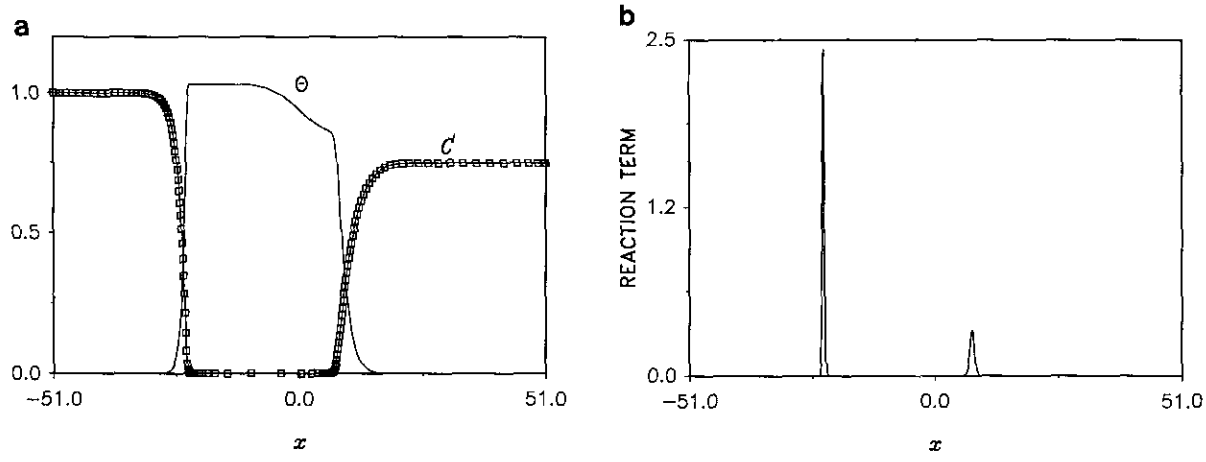

FIG. 3. (a) Θ and C for flames in counterflowing jets, $K = 0.05$. (b) Reaction term for flames in counterflowing jets, $K = 0.05$.

in the x direction and, for the two-dimensional calculations, 64 points in the y direction. The functional (6) is evaluated for the linear combination $0.5\ (\Theta + C)$.

We first illustrate the numerical method for 2 one-dimensional calculations. In Fig. 3a we plot Θ and C as a function of x for $K = 0.05$ and $\phi = 0.75$. The collocation points determined from the adaptively chosen mapping are indicated on the graph of C and demonstrate the high resolution of the two separated layers of the solution obtained by adaptive choice of the mapping (7). In describing the figures we refer to the flame on the left as F_l and the flame on the right as F_r. In this case the flames are relatively separated. The effect of the reduced concentration ($\phi < 1$) on F_r is to cause a reduced burning temperature and a flame front closer to the stagnation line $x = 0$. This can be also seen in Fig. 3b, where we plot the reaction rate terms. The locations of the maxima indicate the locations of maximal chemical conversion of the reactant (i.e., the flame location), and the amplitudes are increasing functions of the burning temperature. There is a transfer of heat from the hotter F_l to F_r; however, it is relatively gradual, indicating only slight interaction between the two flames. We remark that the temperature profile is relatively flat in the burned region directly behind each of the flames.

In Fig. 4 we plot Θ and C as a function of x for $K = 0.30$ and $\phi = 0.75$. Since the flames are closer there is a much stronger interaction between them, which can be seen in the large temperature gradient for the transfer of heat from F_l to F_r. Although the flames are now closely spaced, attempts to compute this solution using (5) led to a noticeable increase in oscillations.

We finally illustrate localized nonplanar flames which can occur in certain parameter ranges. Such flames have been observed in experiments [16]. These localized states arise due to finite amplitude instabilities which occur for K sufficiently small and can be a precursor to a transition to chaos for stretched flames [11, 20]. We have computed such localized states for the diffusional thermal model for counterflowing jets using the mapping (7). Here we present one such calculation with $\phi = 0.95$ and $K = 0.6$. In Fig. 5 we plot the computed flame locations, taken as the maxima of the reaction term, as a function of the transverse variable y. A localized nonplanar state can be seen for F_l while F_r is planar. The planar behavior for F_r is due to the reduced burning temperature associated with the smaller concentration, which leads to a reduced fluid velocity at the location of the flame.

4. EFFECT ON CONDITIONING OF DIFFERENTIATION MATRICES

We next consider the effect of the proposed mapping on the conditioning of Chebyshev pseudo-spectral differentiation. Since differentiation is a linear operator, the operation of differentiating a function by the Chebyshev pseudo-spectral method can be represented by a matrix operation. Specifically, if u is any function and $\hat{u}$ denotes the vector with components $u_j =$

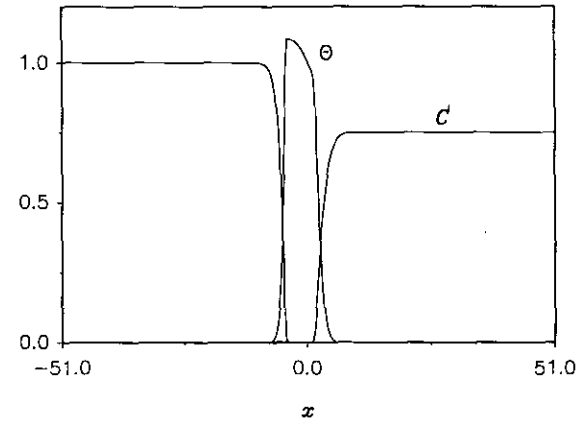

FIG. 4. Θ and C for flames in counterflowing jets, $K = 0.30$.

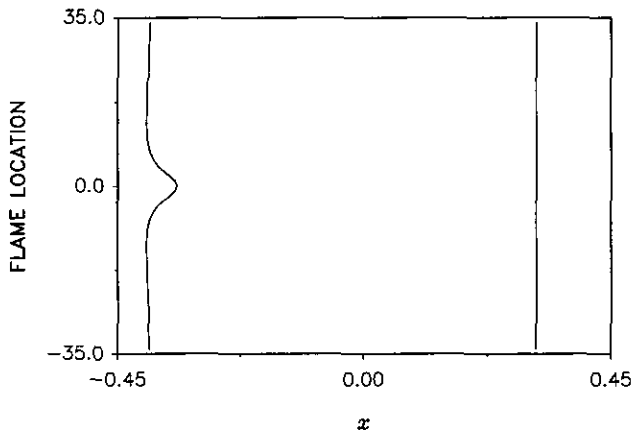

FIG. 5. Flame location as a function of y for localized nonplanar state in counterflowing jets, $\phi = 0.95$, $K = 0.30$.

$u(s_j), j = 0, ..., J$, where s_j are the Gauss–Lobatto points (11), then the operator producing $u'(s_j), j = 1, ..., J$, can be represented by the matrix vector product $D\hat{f}$.

The matrix D is known explicitly and has elements which grow as J^2. While D itself has only the single eigenvalue 0, when appropriate boundary conditions are introduced D has eigenvalues which are $O(J^2)$ [10]. Similarly, the condition number for matrices representing second derivatives is $O(J^4)$. This leads to an ill-conditioning associated with Chebyshev pseudospectral differentiation which results in both severe timestep restrictions and possible loss of accuracy in computing derivatives, e.g., [2, 9, 10, 12, 17, 22, 23].

It appears that this ill-conditioning is related to the clustering of collocation points near the boundary. In [17] a mapping which led to uniformly spaced collocation points in an appropriate singular limit was introduced. It was shown that in this limit the spectral radius of the Chebyshev differentiation matrix was reduced from $O(J^2)$ to $O(J)$, where J is the number of collocation points. However, the effect of a mapping in improving the conditioning of the resulting differentiation matrix must be considered together with the effect of the mapping on the accuracy, in approximating the desired function. It was shown in [7] that the mapping proposed in [17] is not necessarily effective for functions exhibiting layer type behavior.

Here we consider the effect of mappings appropriate to resolve layer behavior, in particular (5) and its extension (7), on the resulting conditioning of the Chebyshev differentiation matrix. When mappings are employed the resulting differentiation matrix can be represented as the matrix product MD, where M is the diagonal matrix with entries ds/dx evaluated at the points (11). In order to illustrate the role of layer type mappings on the conditioning of the matrix, we consider the matrix associated with the second derivative operator with homogeneous Neumann boundary conditions, where we include the boundary condition in the matrix, i.e., an indirect imposition of the boundary conditions. Specifically, we construct the matrix $D_2 = MD\widetilde{MD}$, where $\widetilde{MD}$ is the matrix MD with the first and last rows set to 0. In order to avoid singularities we shift the spectrum of D_2 away from the origin by working with the matrix $D_2' = I - D_2$, where I is the identity matrix.

When the layers are located away from the boundaries the effect of the mapping family (5) (or (7)) is to reduce the clustering of collocation points near the boundaries. This suggests that the computation of such layers may be accompanied by a corresponding improvement in the conditioning of the differentiation matrix. In order to illustrate this point and to give a guide for which layers such improvement is to be expected, we have computed the L_1 condition number $C(D_2')$ for both the mappings (5) and (7). In both cases we specify the location parameters (α_{12} for (5) and α_{12} and α_{22} for (7)). When we employ (5) we compute $C(D_2')$ as a function of α_{11} for the three cases: (i) $\alpha_{12} = 0$; (ii) $\alpha_{12} = -0.5$; (iii) $\alpha_{12} = -0.9$. When we employ (7) we specify $\alpha_{11} = \alpha_{21}$ and compute $C(D_2')$ as a function of α_{11} for the three cases: (i) $\alpha_{12} = -\alpha_{22} = -0.05$; (ii) $\alpha_{12} = -0.5$; (iii) $\alpha_{12} = -\alpha_{22} = -0.9$. For each mapping the effect in cases (i) and (ii) is to expand interior regions at the expense of the boundaries while in case (iii) one or both of the boundary regions is expanded at the expense of the interior (i.e., the clustering of collocation points near the boundaries, in the physical coordinate, is increased relative to the unmapped case).

In Figs. 6 and 7 we plot $C(D_2')$ normalized by the condition number for the unmapped Chebyshev method for (5) and (7), respectively, for the three cases specified above with $J = 120$. Similar results are valid for different values of J. The results demonstrate that a significant improvement in the conditioning of the differentiation matrix can be expected for a wide range of α_{11} (i.e., a range of layer thicknesses). In fact, the values of α_{11} used in practice in our combustion computations lie in the range where such a reduction occurs. Thus, for these values of α_{11}, resolution of the layer has the additional advantage of improving the conditioning of the differentiation matrix. At the

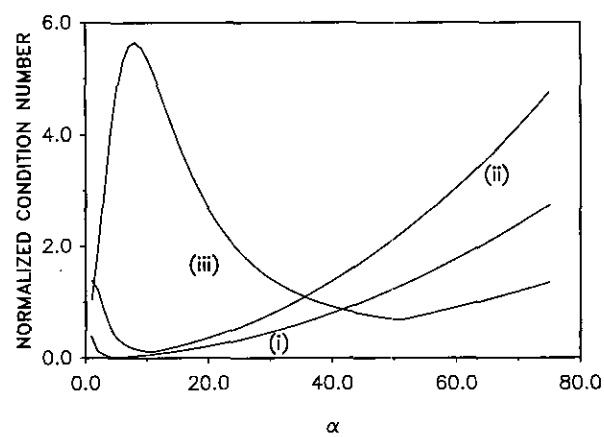

FIG. 6. Condition number for D_2' as a function of α_{11} employing (5). Cases (i), (ii) and (iii) described in text. $J = 120$.

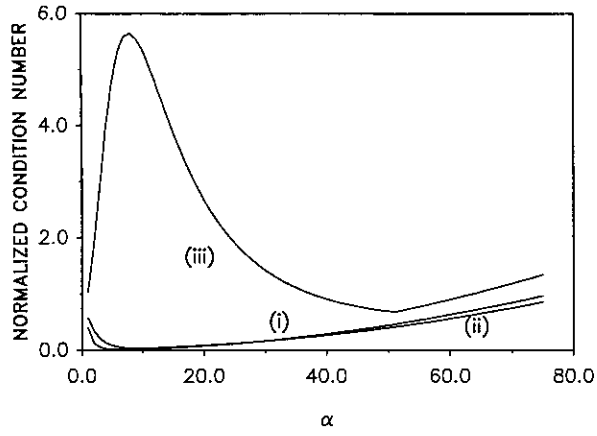

FIG. 7. Condition number for D_2^1 as a function of α_{11} employing (7). Cases (i), (ii) and (iii) described in text. $J = 120$.

minima there is a reduction of nearly two orders of magnitude in the condition number. When the layers are located close to the boundaries (case (iii) for each figure) there is a significant increase in the condition number for moderate values of α_{11}. We conjecture that for these values of α_{11} the overall density of collocation points increases near the boundary leading to the increase in condition number. For larger values of α_{11} the effect of the mapping is to expand layers at the expense of the boundaries, thus resulting in a reduction in the clustering of collocation points near the boundaries. This may be related to reduction in the condition number for this case for larger values of α_{11}.

We next discuss the potential for using mappings to improve the conditioning of Chebyshev differentiation for general functions (i.e., functions not exhibiting layer type behavior). For any particular function, errors in differentiation result from both ill-conditioning of the differentiation operation and approximation errors. While the use of mappings such as (5) and (7) will reduce approximation errors for functions exhibiting layer type behavior, approximation errors can be increased for functions which do not exhibit layer type behavior. However, for (5) the maximal reduction in the condition number occurs for relatively small values of α_{11} ($\alpha_{11} = 5$ for $J = 120$, $\alpha_{11} = 8$ for $J = 256$) for which the layer type nature of the mapping is not pronounced. As a result there may be an overall reduction of the error in Chebyshev differentiation for a wider class of functions than those exhibiting layer type behavior at $x = 0$ (i.e., the reduction in numerical errors due to improved conditioning can be more significant than the increase in approximation error due to the use of a layer type mapping for functions which do not exhibit layer type behavior).

In order to test this we considered the extreme case of the approximation of polynomials x^j, $0 \le j \le J$. When no mappings are employed there is no discretization error; i.e., all of the error in Chebyshev differentiation is due to round off error. When mappings are employed there will be both round-off error and approximation error, as the mapped Chebyshev approximation is no longer exact for polynomials. The approximation error for x^j, which is nonzero when mappings are employed, would be expected to increase with j since x^j varies slowly near $x = 0$ for large j. Thus it would be expected that the use of (5) or (7) as a condition number reducing mapping would lead to an overall reduction in error for a range of j near 0 and an increase in error for a range of values of j near J.

This behavior is illustrated in Fig. 8. The ratio of the maximum norm errors for the fourth derivative of x^j with the mapping (5) ($\alpha_{11} = 5$, $\alpha_{12} = 0$) to the errors without mapping is plotted for $J = 120$. The derivatives are computed using matrix multiplication with a straightforward computation of D using the expression given in [10]; however, the diagonals are adjusted so as to maintain a null row sum as proposed in [2]. It can be seen that errors are significantly reduced for $j \le J_*$, where $J_* \simeq J/4$, an approximate scaling that we have observed for other values of J as well. Similar results (although at much lower values) were found for the approximation of the second derivatives.

Thus, the use of (5) as a condition number reducing mapping can ameliorate round-off error in the computation of higher derivatives. Whether this is effective in any particular application depends on the function being approximated. For polynomials there is no discretization error with the unmapped method while there is a discretization error when mappings are employed. Thus, for sufficiently high degree polynomials the discretization error with the mapping is large enough to overcome the improvement in conditioning. (For functions which are polynomials in $q^{-1}(x, \alpha)$ the opposite is true as there is no discretization error when the mapping is employed.) Neither class of functions would be expected to exactly occur in the solution of a system of partial differential equations; however, the results in Fig. 8 indicate that improvement can occur for a large class of functions, including functions which do not exhibit layer behavior. For functions which do exhibit layer behavior, the results suggest the possibil-

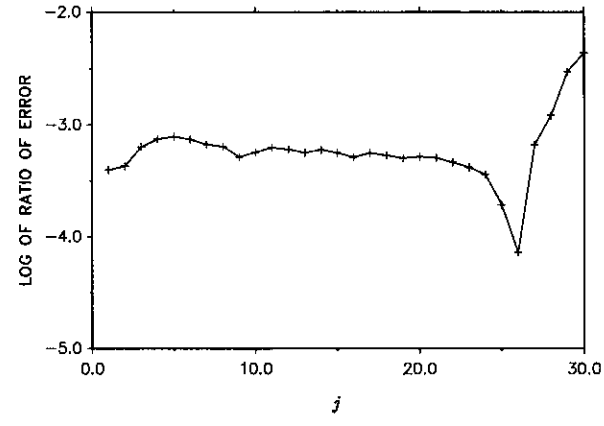

FIG. 8. Logarithm of the ratio of the maximum norm error in the fourth derivative for x^j for the mapped method to the unmapped method. The mapping parameters are $\alpha_{11} = 5$ and $\alpha_{12} = 0$; $J = 120$.

ity that including the condition number as a penalty term in the minimization might be a technique to balance accuracy and conditioning in the resulting adaptive procedure.

REFERENCES

1. J. Augenbaum, *Appl. Numer. Math.* **5,** 459 (1989).
2. A. Bayliss, A. Class, and B. J. Matkowsky, *J. Comput. Phys.* **116,** (1995), in press.
3. A. Bayliss, D. Gottlieb, B. J. Matkowsky, and M. Minkoff, *J. Comput. Phys.* **81,** 421 (1989).
4. A. Bayliss, R. Kuske, and B. J. Matkowsky, *J. Comput. Phys.* **91,** 174 (1990).
5. A. Bayliss and B. J. Matkowsky, *J. Comput. Phys.* **71,** 147 (1987).
6. A. Bayliss, B. J. Matkowsky, and M. Minkoff, *SIAM J. Appl. Math.* **49,** 1421 (1989).
7. A. Bayliss and E. Turkel, *J. Comput. Phys.* **101,** 349 (1992).
8. J. P. Boyd, *Chebyshev & Fourier Spectral Methods,* Lecture Notes in Engineering, Vol. 49 (Springer-Verlag, New York, 1989).
9. K. Breuer and R. Everson, *J. Comput. Phys.* **99,** 56 (1992).
10. C. Canuto, M. Y. Hussaini, A. Quarteroni, and T. A. Zang, *Spectral Methods in Fluid Dynamics* (Springer-Verlag, New York, 1987).
11. A. Class, A. Bayliss, and B. J. Matkowsky, *Appl. Math. Lett.* **6,** 3 (1993).
12. W. S. Don and A. Solomonoff, Accuracy and speed in computing the Chebyshev collocation derivative, preprint.
13. D. Gottlieb and S. A. Orszag, *Numerical Analysis of Spectral Methods: Theory and Applications,* CBMS-NSF Conference Series in Applied Mathematics (SIAM, Philadelphia, 1977).
14. H. Guillard, J. M. Male, and R. Peyret, *J. Comput. Phys.* **102,** 114 (1992).
15. H. Guillard and R. Peyret, *Comput. Methods Appl. Mech. Engrg.* **66,** 17 (1988).
16. S. Ishizuka and C. K. Law, in *19th Symposium on Combustion* (Combustion Institute, Pittsburgh, 1982), p. 327.
17. D. Kosloff and H. Tal-Ezer, *J. Comput. Phys.* **104,** 457 (1993).
18. B. J. Matkowsky and G. I. Sivashinsky, *SIAM J. Appl. Math.* **35,** 230 (1978).
19. K. G. Shkadinsky, G. V. Shkadinskaya, B. J. Matkowsky, and V. A. Volpert, *SIAM J. Appl. Math.* **53,** 128 (1993).
20. G. I. Sivashinsky, C. K. Law, and G. Joulin, *Combust. Sci. Technol.* **28,** 155 (1982).
21. A. Solomonoff and E. Turkel, *J. Comput. Phys.* **81,** 239 (1989).
22. L. N. Trefethen and M. R. Trummer, *SIAM J. Numer. Anal.* **24,** 1008 (1987).
23. J. A. C. Weideman and L. N. Trefethen, *SIAM J. Numer. Anal.* **25,** 1279 (1988).
24. C. K. Westbrook and F. L. Dryer, *Combust. Sci. Technol.* **27,** 31 (1981).